Journal of Hydrology 527 (2015) 494–504

Contents lists available at ScienceDirect

Journal of Hydrology

journal homepage: www.elsevier.com/locate/jhydrol

Analysis and simulation of large erosion events at central Texas unit source watersheds

Chad Furl [a,*], Hatim Sharif [a], Jaehak Jeong [b]

[a] Department of Civil and Environmental Engineering, University of Texas at San Antonio, One UTSA Circle, San Antonio, TX 78249, United States
[b] Blackland Research Center, Texas A&M AgriLife Research, 720 E Blackland Road, Temple, TX 76502, United States

ARTICLE INFO

Article history:
Received 4 June 2014
Received in revised form 29 April 2015
Accepted 11 May 2015
Available online 16 May 2015
This manuscript was handled by Konstantine P. Georgakakos, Editor-in-Chief, with the assistance of Ehab A. Meselhe, Associate Editor

Keywords:
Daily erosion
Long-term erosion
SWAT model
Agriculture erosion
Empirical erosion
Unit source watershed

SUMMARY

This study uses long-term daily sediment records (12–51 years) from 5 unit-source watersheds in central Texas to examine the role of large infrequent erosion events in the makeup of the overall soil loss record. Additionally, multi-decadal daily erosion simulations with the Soil and Water Assessment Tool (SWAT) using both the Modified Universal Soil Loss Equation (MUSLE) and physics based erosion routines are conducted to assess the routine's ability to predict extreme events and long-term budgets. The empirical record indicates the upper 10% of erosion events (in terms of mass) comprise roughly half of the long-term soil loss sum. These upper end events are characterized by large unit flow erosion values and not necessarily associated with precipitation or runoff extremes. The two SWAT routines showed little differences in total soil loss masses; however, the distribution of soil loss events from the physics based simulation, including upper end events, more closely resembled the empirical record than the MUSLE prediction.

1. Introduction

Conducting accurate long-term (decadal plus) simulations of watershed erosion are problematic in part due to the inherent difficulties in developing mathematical descriptions of dynamic soil supply-transport-deposition cycles over space and time (Boardman, 2006; White, 2005; Nearing, 2013). Spatially distributed and continuous catchment models that simulate runoff and erosion have been developed and enhanced over the past few decades with the development in computing processors and geographical information systems. These models allow estimation of soil erosion from complex hydrologic systems characterized by heterogeneous soils, vegetation, and topography over a long period (Merritt et al., 2003). For surface erosion processes, a large portion of the literature has been dedicated to different versions of the empirically developed Universal Soil Loss Equation (USLE). The USLE was originally developed during the 1950s and 60s from greater than 10,000 plot years of data at approximately 50 research stations across the United States (Wischmeier and Smith, 1978). While the USLE has proven successful in many applications, its derivatives, the Revised USLE and Modified USLE (Williams, 1975; Renard et al., 1997), are presently the most commonly used empirical models. Nevertheless, recent efforts have focused more on developing process based models using physically based equations to describe surface processes and sediment routing. Models such as KINEROS (Smith, 1981), EUROSEM (Morgan et al., 1998), and WEPP (Nearing et al., 1989) estimate soil detachment from raindrop energy, sheet flow, and rilling using physical descriptions of detachment theory. The models also benefit from sophisticated descriptions of climate, hydrology, plant growth, and land management. Despite their complexity, physics-based models have shown similar ability to empirical models in predicting long-term soil losses (Bhuyan et al., 2002; Tiwari et al., 2000; Aksoy and Kavvas, 2005).

Model choice aside, there are practical limits placed on modeled predictions related to the natural variability of erosion and errors in field measurements. Few studies exist examining the variability in erosion data, but fairly large coefficients of variation (3–173%) have been reported among replicated plots (Wendt et al., 1986; Ruttimann et al., 1995; Nearing, 2000). The relative difference between replicates tends to decrease as erosion magnitude increases, but the non-unique erosional response from a given storm presents problems for model calibration and assessment of model results.

* Corresponding author. Tel.: +1 360 556 2473.
E-mail address: nfk796@my.utsa.edu (C. Furl).

http://dx.doi.org/10.1016/j.jhydrol.2015.05.014
0022-1694/

Erosion measurements are needed to develop, calibrate, and validate models, but this type of data is woefully inadequate for most parts of the world (Boardman, 2006). Where data are available, they are largely concentrated in the form of standard erosion plots. Analysis of plot data is constructive and necessary; however we should not expect standard plots to provide an accurate depiction of landscape level processes. Plot data are often based on short, relatively linear slopes not representative of the landscape as a whole, and tend to show larger amounts of erosion than may be expected at the field level. This may in part be due to sampling devices at the end of these confined areas increasing flow across the plot driving the erosion rate higher (Evans, 1995).

Lack of long-term empirical data from unit-source watersheds and larger has limited our understanding of decadal plus processes and the role large infrequent meteorological events have on long-term erosion budgets. From the standard plot perspective, Risse et al. (1993) suggests at least 22 years of monitoring are needed to arrive at representative annual values and characterize large infrequent meteorological events. Similarly, Lane and Kidwell (2003) recommend 16 years or greater. Gonzalez-Hidalgo et al. (2009) show a minimum of 100 measured events should be sufficient to capture long-term plot dynamics. These plot studies along with others provide considerable evidence that individual storms can have a large impact on long-term erosion budgets. From the unit-source perspective, Nearing et al. (2007) reported 6–10 storm events produced 50% of the total sediment yield at six rangeland unit-source watersheds (southern Arizona) over an 11 year period. In the seventh watershed studied, two storms produced 66% of the total sediment yield. At nine small cultivated watersheds within the North Appalachian Agriculture Research Station, 5 events produced at least 66% of total soil loss for each of the unit-source watersheds over 28 year timespan (Edwards and Owens, 1991). Watershed sizes in these unit-source studies ranged from 0.2 to 5.4 ha.

Recognition of the importance of extreme erosion events is easy to identify in the field and through the analysis of adequate empirical records; however, relatively little attention has been given to the subject from the modeling community. The USLE was designed and has mainly been used to find average rates over long periods of time ignoring the individual events contributing to the rate (Boardman, 2006). If large scale erosion events are in fact the dominant force behind erosion budgets at the catchment level, their recognition in erosion models is necessary to arrive at reasonable conclusions. Watersheds in arid-semiarid regions subject to infrequent high intensity events would have the most to gain from analysis of individual rainfall/runoff events in the construction of long-term records.

In the present study, we analyze daily soil erosion records at 5 unit-source watersheds from the Grassland, Soil, and Water Research Laboratory located near Riesel, Texas (herein "Riesel watersheds"). Three land use types are examined including row crops, hay production, and native prairie. The length of the erosion records range from 12 to 51 years and are among the longest continuous records in the world for unit-source sized watersheds. Objectives of the study are to (1) discern the impact of large erosion events on long-term sediment budgets and describe their temporal and land use characteristics and (2) assess the ability of empirical and physics based routines to predict long-term budgets and large erosion events.

2. Methods

2.1. Site information

The Riesel watersheds were established by the United States Department of Agriculture – Soil Conservation Service (USDA-SCS) to examine soil and hydrology responses to various agricultural land management practices (Fig. 1). The station began collecting data in the late 1930s and is the only original USDA experimental watershed still in operation today. Presently, the Riesel and other experimental watersheds around the US are managed by the USDA Agricultural Research Service (ARS). Research at the Riesel watersheds has been used in the development of several hydrologic and erosion models (EPIC/ALMANAC, APEX, SWAT) and has been instrumental in shaping modern agricultural practices across the central Texas region (Williams et al., 2008). There are numerous published reports using data from the watersheds including works on precipitation and weather (Harmel et al., 2003), runoff processes (Allen et al., 2005; Arnold et al., 2005; Harmel et al., 2006), soil erosion (Allen et al., 2011; Harmel et al., 2006; Wang et al., 2006), and the sampling network (Harmel et al., 2007). Previous analyses of soil erosion have focused attention on monthly or annual data. A brief description of the watersheds pertinent to the current study is described below. Readers requiring additional detail on specific aspects of the network are asked to refer to works cited above.

Five watersheds were selected for analysis based on continuity of a daily erosion record, size (1–10 ha), and land use type (Fig. 2; Table 1). Each of the watersheds contains a single land use and represents edge of field erosion processes. Watersheds Y6, Y8, and Y10, have remained cultivated under conservational methods with contoured rows, terraces, and grassed waterways over the length of the erosion record (Allen et al., 2011). These watersheds have primarily been used to produce corn/sorghum during the warm season and wheat/oats for overwinter crops. Watershed W10 has been used for grazing and/or haying, while SW12 has been maintained as a remnant native prairie. Management records are available for a subset of the erosion record.

2.2. Environmental characteristics

Long hot summers and short mild winters are typical across the central Texas region with a warm annual growing season from mid-March to mid-November. Mean annual rainfall over the period of record is between 880 and 900 mm. Spring (April, May, June) and Fall (October, November, December) are the wettest seasons followed by Winter (January, February, March) and Summer (July, August, September) (Harmel et al., 2003). The majority of rainfall can be attributed to passage of continental fronts, while convective events during warmer months contribute short-duration high intensity events. Occasionally, tropical disturbances protrude far enough inland resulting in major precipitation events (Asquith and Slade, 1995).

Houston Black (Vertisol) soils containing an approximate size distribution of 17% sand, 28% silt, and 55% clay dominate the watershed. The soil erodibility factor (K) for this clay rich soil is 0.32 $(0.013\ \text{metric ton} * \text{m}^2 * \text{h})/(\text{m}^3 * \text{metric ton} * \text{cm})$. Sheet and occasional rill erosion are the dominant soil detachment and transport mechanisms observed at the site. The soil series consists of moderately well drained, deep soils formed of weakly consolidated calcareous clays and marls. The soils have a high shrink swell capacity allowing for high infiltration rates when dry due to preferential flow through surface cracks and very low hydraulic conductivity when saturated (hydraulic conductivity $\approx 1.5\ \text{mm h}^{-1}$). Allen et al. (2005) describe distinct seasonal soil phases affecting flow in the clay terrain. Soils are (1) extensively cracked mid-summer to fall (2) at field capacity late fall to winter (3) experiencing crack closure and lateral groundwater flow from late winter to late spring and (4) below field capacity beginning to crack from early spring to summer. The majority of surface runoff occurs from December–June when the soils are holding more water and cracks are closed. During the summer and fall months there is

Fig. 1. Aerial image of Riesel experimental watersheds (left); native prairie site (right).

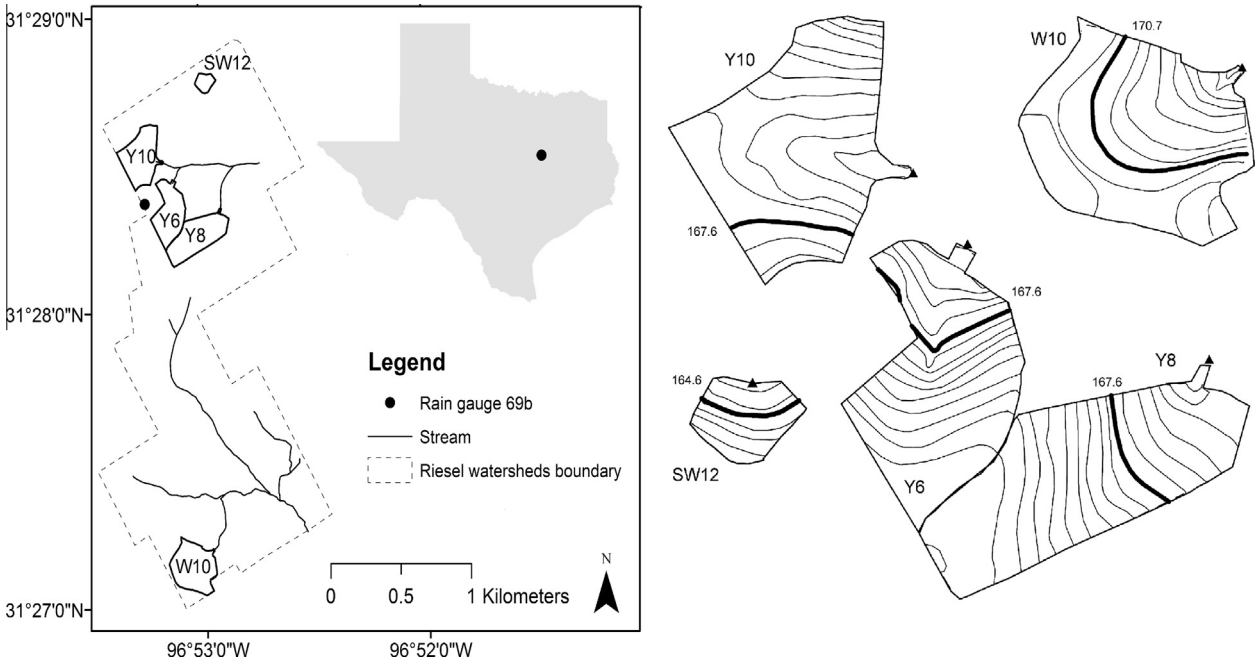

Fig. 2. Riesel watersheds area map.

Table 1
Watershed descriptions with 0.6 m (2 ft) contours for study catchments. The elevation (m) of the bolded line is shown along with outlets (Δ).

Watershed	Size (ha)	Land use	Slope (%)	Daily erosion record (y)
Y6	6.6	Row crop	3.2	51
Y8	8.4	Row crop	2.2	44
Y10	7.5	Row crop	1.9	46
W10	8	Hay	2.6	37
SW12	1.2	Native prairie	3.8	12

much less potential for runoff when high infiltration rates exist. Baseflow from these watersheds is virtually nonexistent accounting for very small percentages of yield (Allen et al., 2005).

2.3. Data collection

Data collected at the Riesel watersheds have grown to a large database of weather, hydrology, land use, and erosion (http://www.ars.usda.gov/Research/docs.htm?docid = 9697). Daily erosion, flow, precipitation, and land use records for each of the five watersheds were compiled from 2012 as far back as the daily erosion record remained continuous. Records range from 12 to 51 years with flow and precipitation values available for each day of erosion.

Runoff and soil loss data were collected under several methods due to the length of the record. Runoff stations mark the outlet of each watershed and are equipped with three stage recording devices. Flow levels are recorded in a stilling well located in the flume or weir structure, and discharge rates are calculated from a known stage-discharge relationship. Historically, float gauges and pressure transducers were the main stage recording device. Since 2001, a bubbler associated with an automatic ISCO sampler has been used as the primary stage recording device with the others remaining as backups.

Currently, an ISCO sampler used to collect runoff for sediment concentrations is triggered on the rising limb of the hydrograph taking flow weighted samples. From 1970s to 2001, automated mechanical Chickasha samplers activated by floats were used to collect samples for sediment analysis (Allen et al., 1976). Prior to 1970s, on-call personnel were used to obtain grab samples for soil loss estimates. Sediment loads are calculated by drying and weighing soil from samples and recording flow during sampling (Harmel et al., 2006). Detection limits for automated sampling of soil loss were 0.000247 t ha^{-1} and 0.00254 mm for flow.

Historical data for 57 rain gauges are available from the Riesel network. A single rainfall record consisting of hourly data were

used in the analysis (and model forcing). The record was constructed by aggregating breakpoint data for three separate tipping bucket rain gauges. RG69b served as the primary rain gauge (>95% of data) with RG75a and 84a serving as backups (Fig. 2). Backup precipitation samples were used when the primary rain gauge was not functioning correctly (reporting daily totals only) or when daily precipitation was 20% different from the mean of the other gauges.

2.4. Model setup and calibration

The Soil and Water Assessment Tool (SWAT) was selected to evaluate surface erosion routines. SWAT is a continuous time model that operates on daily or sub-daily timesteps. SWAT was chosen due to its partial development (original calibration site) at the Riesel watersheds and capacity for calculating soil loss using both empirical (MUSLE and USLE) and physics based techniques. Watershed discretization was lumped with one land use, soil type, and slope. Excess rainfall was calculated using the Green-Ampt Mein-Larson infiltration method, evapotranspiration by the Priestley-Taylor method, and Manning's equation for overland flow and stream routing. Timestep for the physics based erosion model was hourly. For the USLE based erosion techniques, infiltration calculations are conducted at an hourly timestep and routing is aggregated to daily. Theoretical documentation of the model can be found with Neitsch et al. (2011).

The Modified USLE (MUSLE) incorporated into SWAT was developed during the 1970s at 18 small watersheds from Riesel and Hastings, Nebraska (Williams, 1975). Its primary difference from the USLE is replacing the rainfall energy factor with a runoff factor thereby implicitly accounting for soil moisture and runoff production. The equation is given by:

$$\mathrm{Sed} = 11.8 * (Q_{surf} * q_{peak} * \mathrm{area})^{0.56} * K * C * P * \mathrm{LS} * \mathrm{CFRG} \quad (2.4.1)$$

where Sed – soil transported to stream (metric ton day^{-1}), Q_{surf} – surface runoff volume (mm ha^{-1}), q_{peak} – peak runoff rate ($m^3\ s^{-1}$), area – area of watershed (ha), CFRG – coarse fragment factor (unitless). The remaining factors were developed as part of the original USLE: K-soil erodibility factor (0.013 metric ton * m^2 * h)/(m^3 * metric ton * cm), P – Practice factor (unitless), and LS – Length/slope factor (unitless). The cover and management factor (C – unitless) is updated daily.

To accommodate the needs of event based modeling, sub-daily algorithms for flow (Jeong et al., 2010) and erosion/sediment transport (Jeong et al., 2011) were recently incorporated into the SWAT model. The surface erosion routines consider both splash and rill erosion (herein "physics based" routines). Splash erosion is modeled from the kinetic energy of rainfall using methods proposed by Brandt (1990). The routine is used in the erosion model EUROSEM and is given by:

$$D_R = k * \mathrm{KE} * e^{-\psi h} \quad (2.4.2)$$

where D_R – soil detachment by rainfall impact (g * m^{-2} * s^{-1}), k – index of soil detachability (g * J^{-1}), KE – total kinetic energy of rain (J * m^2), ψ – calibration exponent (unitless), h – surface runoff depth (mm). The kinetic energy term is partitioned into energy from direct throughfall and leaf/stem drainage.

Overland (rill and interrill) flow erosion routines are adopted from the ANSWERS model and are a function of average bed shear stress, crop management, and soil erodibility. The equation is given by:

$$D_F = 11.02 \alpha K C \tau^{\beta} \quad (2.4.3)$$

where D_F – flow erosion rate (kg * m^{-2} * h^{-1}), τ – average bed shear stress (N * m^{-2}), α/β – calibration parameters (unitless), K – flow erodibility factor, C – Crop factor.

Erosion and flow parameters were calibrated using the parameter estimation software PEST (Version 13). PEST is a model independent parameter estimator using the Gauss–Marquardt–Levenberg (GML) method for non-linear models. The relationship between model output (X), input parameters (p), and observations (H) is given by:

$$Xp = H \quad (2.4.4)$$

The goal of PEST is to find the p that minimizes the objective function through model iterations. PEST defines the objective function as the sum of squared deviations between model output and experimental observations:

$$\Phi = (H - Xp)^{t} Q (H - Xp) \quad (2.4.5)$$

where Q is proportional to the covariance matrix of measurement noise and t indicates the matrix transpose operation. Φ is related to the root mean square error (RMSE) by:

$$\mathrm{RMSE} = (\Phi * N^{-1})^{.5} \quad (2.4.6)$$

The relationship between model inputs and outputs is linearized by formulating a Taylor expansion about the best parameter set prior to each iteration. The linearized problem is then solved for new parameters and the model is run again. Φ is minimized when:

$$P = (X^{t} Q X)^{-1} X^{t} Q h \quad (2.4.7)$$

To reduce problems associated with overfitting or unrealistic parameter inputs, models were first manually calibrated according to methods proposed by Engel et al. (2007). Once reasonable ranges of input parameters were identified PEST optimization was completed (flow before erosion). For erosion calibration, fixed terms from the MUSLE were combined such that:

$$\mathrm{Sed} = b * C * (Q_{surf} * q_{peak} * \mathrm{area})^{0.56}. \quad (2.4.8)$$

The C factor is updated daily by:

$$C = \exp\{[\ln(0.8) - \ln(C_{mn})] * \exp(-0.00115 * \mathrm{rsd}_{surf}) + \ln(C_{mn})\} \quad (2.4.9)$$

where C_{mn} – minimum value for C, rsd_{surf} – amount of residue on soil surface (kg ha^{-1}).

Input parameters chosen for calibration were harvest index, C_{mn}, residue decomposition rate, and the linear factor b. SWAT calculates surface residue creation (rsd_{surf}) through a harvest index which is the percentage of above ground biomass left after harvest. Surface residue is updated daily by a decomposition rate. Harvest index and decomposition rate were calibrated for each plant type. The model treats residue from all crops the same in terms of erosion abatement (Eq. (2.4.9)).

Using a similar approach of combining fixed terms (Eq. (2.4.8)), the rill/interrill physics based equation is given by:

$$\mathrm{Sed} = b * \tau^{\beta} \quad (2.4.10)$$

Calibration parameters selected for adjustment were b, β, and ψ (Eq. (2.4.2)). Once PEST iterations were completed, model erosion results were tuned linearly by the b factor to match total yield over calibration time period. This lowered model performance statistics (shown Section 5.1), but provided a more realistic representation in terms of overall soil loss mass. Selection of flow calibration parameters were guided by Arnold et al. (2012). The most sensitive flow parameters were curve number, available soil water content, and evaporation compensation factor. Watersheds Y6, Y8, Y10, and

Table 2
Erosion record information.

	Y6	Y8	Y10	W10	SW12
Daily erosion	1962–2012 (51)	1969–2012 (44)	1967–2012 (46)	1976–2012 (37)	2001–2012 (12)
Management data	1982–2012 (31)	1983–2012 (30)	1982–2012 (31)	NA	NA
No of events	237	276	311	134	102
% of Flow events with erosion measurements	7.6	12.1	17.4	10.7	26.2
Avg no yearly events (d)	4.6	6.3	6.8	3.6	8.5
Standard deviation (d)	5.1	4.5	5.9	4.2	7.5
Max (d)	25	23	29	22	25
Min (d)	1	1	1	1	1

W10 were calibrated from 1990 to 2001 and validated from 2002 to 2012 using daily results. At SW12, the calibration period was 2002–2006 and validation from 2007 to 2012.

2.5. Data analysis

Sediment yield frequency distributions over the period of record are constructed by sorting erosion values and computing total sediment yield as a function of percentage of erosion events contributing. The upper 10% of sediment yields from this ranking procedure is referred to throughout as "upper end" events. This threshold was chosen as it has been shown to account for roughly 50% or greater of long-term soil loss budgets in other studies (Gonzalez-Hidalgo et al., 2009; Nearing et al., 2007; Edwards and Owens, 1991). Coefficient of determination (r^2) values from least squares regression are provided describing the amount of variance in the daily erosion record explained by daily rainfall, maximum 1-h rainfall, daily flow, and their combinations ($p < 0.05$). Adjusted r^2 values are reported for least squares multiple regressions. A simple erosion index is used to understand the erosive efficiency of events. The index is calculated by dividing the erosion event by daily flow (t ha^{-1} mmflow^{-1}). Boxplots shown throughout the manuscript display the median, interquartile range, and whiskers extend to $q_{1,3}$ +/−1.5(q_3–q_1).

Model simulations (flow and erosion) were evaluated using NSE, PBIAS, and r^2 efficiency statistics calculated from daily results. Formulas for these commonly used evaluation statistics can be found with Moriasi et al. (2007). Model output values smaller than the empirical limit of detection were set to zero. Analysis of the distribution of simulated erosion results was conducted to draw comparisons with the empirical record and examine the ability to produce upper end events. To compare distributions, number of daily events and mass of values above the limit of detection, 10th percentile, median, and 90th percentile of the empirical record were extracted. These values, defined by the empirical record, were then applied to the model results to calculate count and mass of soil lost over varying thresholds. An example is provided for Y10 in the discussion.

3. Event erosion

3.1. Occurrence and magnitude

1060 daily erosion measurements were recorded from 190 gauge years; continuous records at the watersheds ranged from 12 to 51 years. Events per year were correlated with annual rainfall amounts (0.77) and highly variable between years ranging from 1 to 29 (Table 2). Approximately 70% of erosion events occurred from January to June.

Percent of flow events with accompanying erosion measurements ranged from 7.6% to 26.2% and suggests greater sensitivity under the ISCO sampling years. SW12 was the only basin sampled completely with the ISCO and contained the highest percentage of flow values with erosion events. Y6, Y8, Y10, and W10 watersheds produced larger events per year and lower medians during the ISCO sampling years. No attempt was made to construct a complete erosion record in part due to the differential erosion response at a given flow (Section 3.2).

Daily soil loss measurements ranged from 0 to 5.31 t ha^{-1} with approximately 70% of the non-zero measurements less than 0.1 t ha^{-1} (Fig. 3). Median values were highest in the row cropped basins (0.04–0.07 t ha^{-1}), and about an order of magnitude lower in the hay and prairie basins (0.008 and 0.005 t ha^{-1}, respectively). Frequency distributions indicated the upper end events accounted for about 40–60% of long-term yields (Fig. 3). Basins Y8 and Y10 showed the largest disproportionate impact from upper end events producing greater than 60% of long-term yields. Upper end events at Y6 and SW12 both resulted in approximately half of long-term erosion rates, and upper end events at the hay watershed produced 43% of overall mass. The frequency distribution shape at SW12 was similar to the other basins despite its record solely coming from the most recent instrumentation. On average, events comprising the upper half of total sediment yield occurred once every 2.5 years. The cumulative impact of upper end events is very similar to those found over shorter time periods at ARS unit-source watersheds in Arizona and Ohio along with experimental plots across the central and eastern US (Nearing et al., 2007; Edwards and Owens, 1991; Wischmeier and Smith, 1978).

3.2. Precipitation and flow characteristics

Coefficient of determination (r^2) values for least squares regression relating erosion to daily precipitation, daily flow, maximum 1-h precipitation and their combinations are shown in Table 3. Daily flow was the best independent variable for the single variable equations explaining on average about one quarter of the variance in erosion events. Combinations of flow and precipitation (both daily and 1-h maximum) performed similarly. Allen et al. (2011) reported a very high r^2 value (0.97) between runoff and erosion at the Y2 watershed during the Texas drought of record (1948–1953). The Y2 watershed (53 ha) drains watersheds Y6, Y8, and Y10. The authors noted the relationship was similar to empirical equations typical of bare soil conditions developed by others. Nearing et al. (2007) showed strong correlations ($r > 0.8$) for erosion and runoff volume at the desert shrub sites in southern Arizona previously mentioned.

The small r^2 values encountered over the period of record underscore the impact of seasonal land use, weather, and hydrology; long-term climate and cover responses, along with natural variability, and measurement uncertainty (10–21%; Harmel et al., 2009). Results also suggest the common practice of estimating event loads from flow in order to fill gaps of an empirical record may not be appropriate. In general, erosional responses to a given flow could span two orders of magnitude. The distributions of flow and precipitation events resulting in erosion are shown in Fig. 4

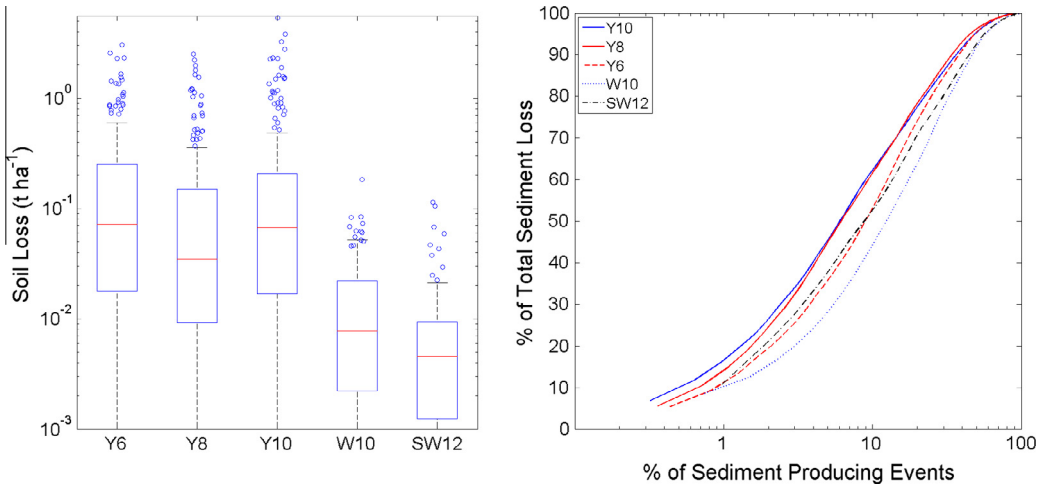

Fig. 3. Daily erosion boxplots (jittered values are upper end events) and cumulative sediment yield versus percent of events required to produce yield.

Table 3
Coefficient of determination values (r^2) for linear regression ($p < 0.05$) related to daily erosion.

	Flow	Precipitation	Max precipitation[a]	Flow-precipitation	Flow – max precipitation	Precipitation – max precipitation	Flow – precipitation – max precipitation
Y6	0.17	0.14	0.21	0.20	0.25	0.22	0.25
Y8	0.23	0.19	0.16	0.25	0.25	0.20	0.26
Y10	0.22	0.19	0.18	0.25	0.27	0.21	0.27
W10	0.29	0.18	0.13	0.29	0.29	0.17	0.29
SW12	0.21	0.06	0.11	0.20	0.20	0.11	0.19

[a] Maximum 1-h precipitation.

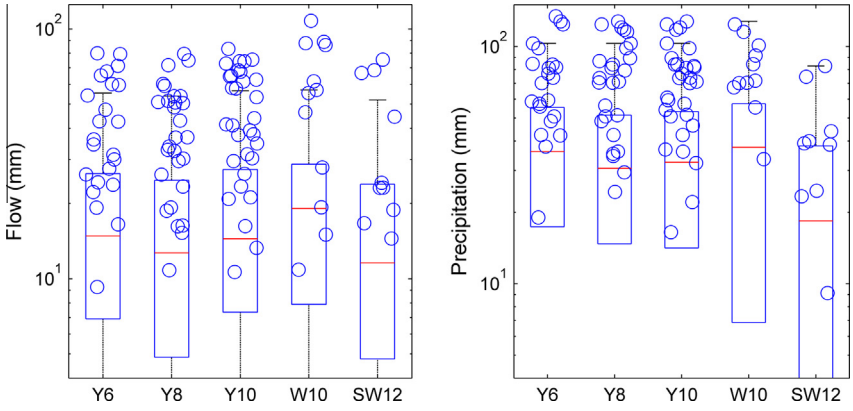

Fig. 4. Flow and precipitation boxplots for erosion days (jittered points represent upper end events).

along with precipitation and flow for upper end events. At all sites, upper end events were generated at precipitation and flow amounts near or below the median up to the upper end of the distribution. The average upper end event occurred at the 80th percentile of flow and precipitation distributions.

4. Erosion index

To examine the temporal and land use patterns associated with upper end events, an erosion index was created by normalizing erosion results by flow (t ha^{-1} mm$_{\text{flow}}^{-1}$). Upper end events held high index values (around 90th percentile of erosion indices) at each of the watersheds suggesting they are characterized by efficient transport and not necessarily extreme flow or precipitation (Fig. 5). This is somewhat surprising given the chance of low flow values (denominator) to produce large indices. Similar to erosion mass, index magnitudes were approximately an order of magnitude higher at row crop basins compared to the hay and prairie basins.

4.1. Temporal characteristics of upper end events

Harmel et al. (2006) describe a monthly erosion pattern at selected Riesel watersheds similar to the temporal flow pattern. Greater monthly soil losses were experienced during the spring and winter months with little soil loss during fall and summer months. Fig. 6 shows erosion indices by month plotted with upper end events. At the row cropped basins, erosion indices were at

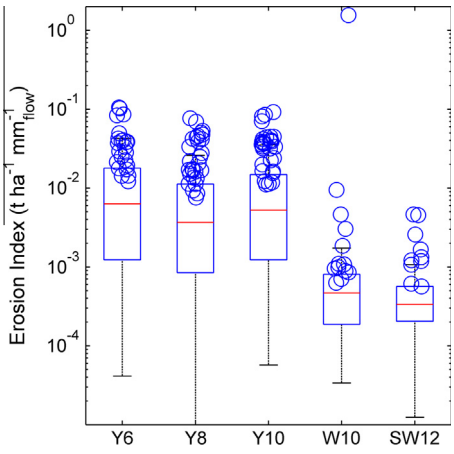

Fig. 5. Erosion index boxplots (jittered points are upper 10% events).

their maximum during March, April, and May with approximately 70% of the upper end events occurring between March and June. Clearly, the watershed's ability to produce flow during the spring months is necessary for erosion to occur; however, the erosion index was not correlated with an antecedent precipitation index ($r \approx 0$) (Kohler and Linsley, 1951). The lack of an erosion index/antecedent precipitation index correlation is in part due to a second spike in the erosion indices during the driest portion of the year in August and September. Allen et al. (2011) found erosion indices were 2.5 times higher during periods of drought than long-term averages. The authors attributed this to rill network development, piping, and tendency to form easily entrained aggregates during drought. Regardless of the physical mechanism, summer and fall events show an increased efficiency to deliver soil during flow events but comprise a small percentage of upper end events (<10%) and total loads. Erosion indices at W10 and SW12 displayed a similar but subdued pattern to the row crop basins. However, upper end events were not concentrated in the spring time at the sites. At both sites, soil loss was greatest during winter months and upper end events fairly evenly spread across non-summer months.

4.2. Land use characteristics of upper end events

Table 4 provides information on the timing and occurrence of agricultural practices at the row cropped basins along with erosion sums by crop type. The data were compiled from 1982 to 2012 (Y8, 1983–2012) when complete management records were available. Typical rotations involved two seasons of warm annuals followed by a cool annual. Fields were left fallow the entire year in 2001.

Crop erosion indices were approximately an order of magnitude higher for warm annuals than cool annuals (Fig. 7). Harmel et al. (2006) points out a similar pattern between crop types in monthly results. Median erosion indices for fallow/residue cover conditions were lower than warm annuals, but showed the ability to produce upper end events. Little difference existed between indices for warm and cool residues. Residue surface erosion sums approximately equaled erosion under warm season crops even though residue conditions persisted about twice as much. Fields were left fallow in 2001 and produced greater than 10% of the 30 year record along with 2 upper end events at each basin. All upper end events with the exception of 1 were confined to residue or warm annual land uses.

An example of the differential erosional response by crop type is provided during the warm annual growing season of 1991. Y10 and Y8 were both planted with corn in March and harvested in late August. Winter wheat was planted on Y6 in November of 1990 and harvested in May the following year. During April and May of 1991 Y10 and Y8 experienced 5 and 6 erosion events, respectively including 2 upper end events. Storms during these 2 months accounted for approximately 10% of their 30 year record (Table 4). Y6 had no erosional response to the series of storms over the two months.

5. Erosion simulation analysis

5.1. Model performance results

The SWAT model adequately simulated flow during the calibration period with both NSE and r^2 values around 0.5 and 0.6, respectively (Table 5). Slightly better performance statistics were

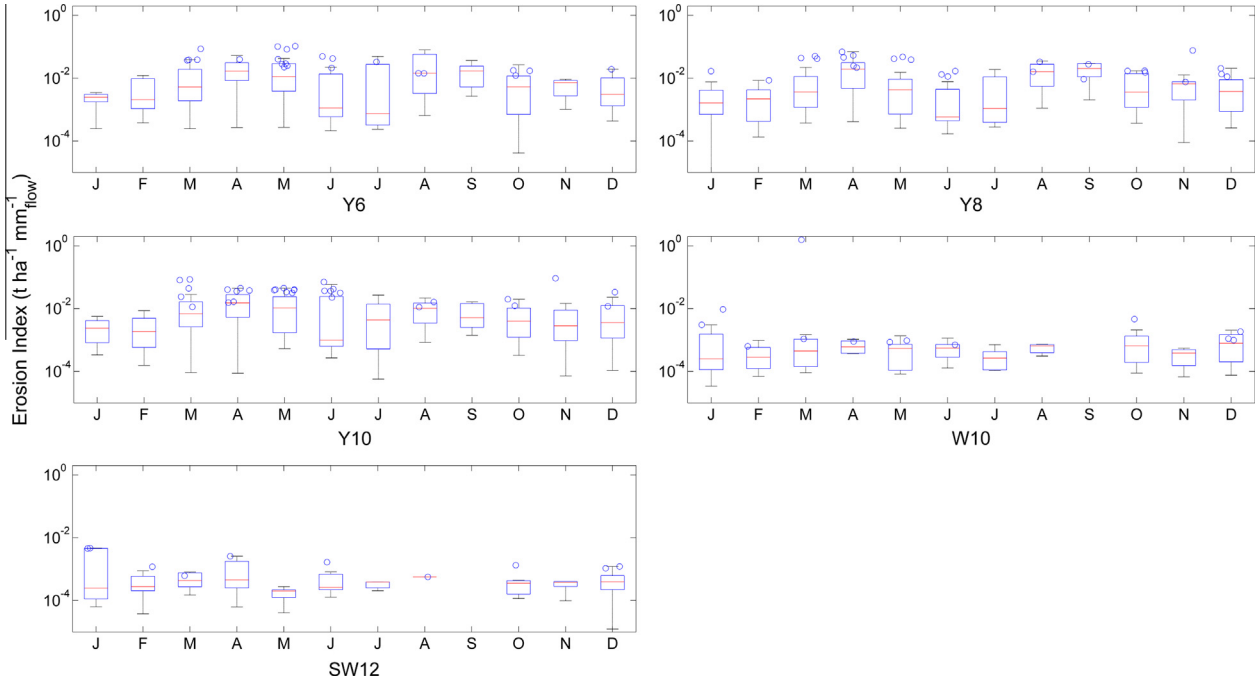

Fig. 6. Erosion index by month (jittered values are upper end events).

Table 4
Crop representation/timing and soil loss.

Surface	Y6 %	Y8 %	Y10 %	Plant	Harvest	Plant to harvest (d)	*n*
Residue	56.4	53.5	54.2	–	–	–	–
Corn	16.9	20.2	18.1	21-Mar	18-Aug	150	45
Sorghum	5.1	5.3	3.7	26-Mar	14-Aug	141	15
Oats	1.9	3.4	9.2	28-Oct	18-May	202	8
Wheat	13.0	15.3	10.6	1-Nov	29-May	209	21
Hay	4.2	2.4	4.2	27-Apr	18-Aug	113	9
Sudan	1.1	–	–	6-Apr	25-Jul	110	2
Cotton	1.4	–	–	14-Apr	20-Sep	159	1

	Soil loss (t ha^{-1})		
	Y6	Y8	Y10
Warm annual	6.9	11.7	11.7
Warm residue	5.0	4.5	5.0
Cool annual	2.0	0.4	2.9
Cool residue	3.3	5.8	4.0
Fallow	3.3	3.7	2.7
Sum	20.4	26.0	26.2

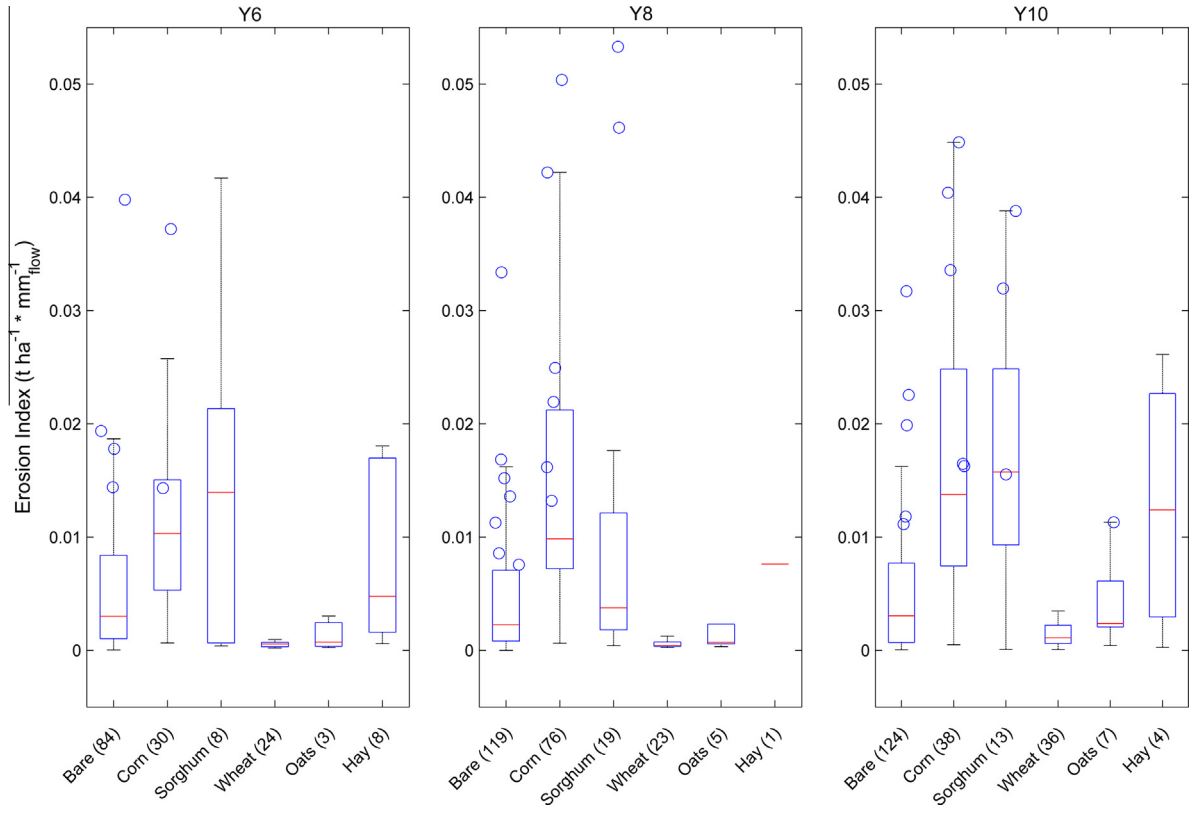

Fig. 7. Erosion index by agricultural land use type.

recorded during the validation period. Aggregated to monthly values, both NSE and r^2 values averaged over 0.75, during calibration and over 0.8 during validation. There was a slight underestimation of spring time flows and overestimation of winter flows for the calibration period. For soil loss, the MUSLE performed as well or better than the physics based routines based on r^2 and NSE values during calibration. During validation, r^2 and NSE values were consistently better using the physics based routines. Little difference was apparent between long-term erosion sums over the validation period which is consistent with other studies comparing USLE derived models with physics-based techniques at plot settings (Shih and Yang, 2009; Tiwari et al., 2000). Both routines underestimated erosion at the row crop basins and had sums very close to the empirical record at the hay and prairie sites.

Owing to the general lack of literature focusing on daily results, there are few data available to contrast daily erosion NSE and r^2 performance statistics. In a review of reported ranges and values of hydrological model performance statistics, Moriasi et al. (2007) included two works calculating daily NSE for soil loss. The better performing model achieved an NSE of 0.11 and 0.23 during calibration and validation, respectively. Wang et al. (2006) reported and average NSE and r^2 value of around 0.55 on monthly results over a 4 year validation period at Y6, Y8, and Y10. Erosion simulations were conducted using the EPIC model. In their

Table 5
Performance statistics for flow and erosion models.

Flow					
Watershed	Empirical yield (mm)	SWAT yield (mm)	NSE	r^2	PBIAS
Calibration					
Y6	1765	2014	0.43	0.6	−14.1
Y8	1945	1765	0.4	0.52	−9.3
Y10	2292	1901	0.58	0.63	17.1
W10	1703	1644	0.45	0.53	3.5
SW12	1450	1530	0.65	0.66	−5.6
Validation					
Y6	1914	1776	0.55	0.57	7.1
Y8	1745	1611	0.51	0.55	7.6
Y10	2243	1561	0.52	0.52	36.1
W10	1246	1625	0.45	0.58	−30.4
SW12	449	522	0.71	0.74	−16.2

		Soil loss – physics based				Soil loss – MUSLE			
Watershed	Empirical yield (t ha^{-1})	SWAT yield (t ha^{-1})	NSE	r^2	PBIAS	SWAT yield (t ha^{-1})	NSE	r^2	PBIAS
Calibration									
Y6	9.66	9.66	0.19	0.28	0.0	9.66	0.20	0.20	0.0
Y8	16.26	16.26	−0.48	0.14	0.0	16.26	0.15	0.15	0.0
Y10	14.81	14.81	0.15	0.24	0.0	14.81	0.15	0.15	0.0
W10	0.52	0.52	−0.01	0.09	0.0	0.52	0.06	0.07	0.0
SW12	0.57	0.57	−0.19	0.09	0.0	0.57	0.02	0.14	0.0
Validation									
Y6	8.23	2.35	0.21	0.24	71.4	2.23	0.07	0.15	72.9
Y8	7.69	3.50	0.37	0.37	55.0	6.87	0.17	0.17	10.6
Y10	10.68	6.44	0.25	0.26	39.6	5.47	0.16	0.20	48.7
W10	0.58	0.56	0.09	0.10	3.2	0.54	0.03	0.03	7.1
SW12	0.44	0.55	0.09	0.30	−22.9	0.53	−0.04	0.23	−18.3

presentation of the physics based erosion algorithms for SWAT, Jeong et al. (2011) reported an NSE of 0.92 for calibration in 2001 and 0.16 during validation in 2002.

5.2. Model erosion distributions

Distributions of simulated erosion results were compared to the empirical record by examining number of events and cumulative masses of values above thresholds defined by the empirical record. Results over the limit of detection (LOD-0.000247 t ha^{-1}), 10th percentile, median, and 90th percentile were selected as thresholds. For example, during the validation period at Y10, 116 erosion values were recorded. 90% of the measurements were greater than 0.0033 t ha^{-1} (n = 104), half greater than 0.035 t ha^{-1} (n = 58), and 10% greater than 0.25 t ha^{-1} (n = 12). 99.8 percent of the cumulative mass measured during the validation period was contained in measurements over 0.0033 (upper 90% of measurements), 94% of mass occurred in measurements over 0.035 (upper 50% of measurements), and 51% of the mass was contained in measures over 0.25 t ha^{-1} (upper 10% of measurements). Fig. 8 shows count and cumulative mass comparisons for these empirically defined thresholds for all watersheds during model validation.

The physics based routines did a better job than the MUSLE in identifying the timing and number of overall erosion events. This is in part due to the demand placed upon the MUSLE to produce erosion with each flow event. Even after setting modeled values below the empirical LOD to zero a large discrepancy in counts exists. It is reasonable to assume this discrepancy is magnified by difficulty in obtaining a complete erosion record near the limit of detection. Regardless, MUSLE model output showed large count overestimates at the upper 90th percentile as well. Number of events over the median were similar to the empirical record, but the model was unable to consistently produce upper 10 percentile events. The physics based methods were better able to replicate the correct number of counts at different thresholds of the empirical record including upper 10 percentile events.

Model overestimation of low values and underestimation of high values are an inherent part of USLE derived erosion models due to their deterministic nature and the distribution of natural systems (Nearing, 1998). This has implications for how the mass of the overall long-term record is distributed across event magnitudes. Similar to the long-term frequency distributions, the upper 10% of events accounted for about half of overall erosion during calibration and validation time periods for the row crop and prairie watersheds. Greater than 90% of soil losses at these sites were contained in values above the median. Overall, the physics based approach was better suited at apportioning mass correctly across the distribution. At the row crop sites, physics based methods contained on average 86% of mass over median values and 36% in the upper 10% for calibration and validation combined. For the MUSLE, mass over median and upper 10 percentile for calibration and validation were 51% and ≈0%, respectively.

This notable discrepancy in model performance can also be attributed in the treatment of the exponential multipliers used in the erosion Eqs. (2.4.8) and (2.4.10). The MUSLE estimates erosion as a function of USLE coefficients along with daily and peak runoff multiplied exponentially by 0.56. The physics based routines contain an exponential multiplier (β, calibration parameter) of shear stress created along the rill network. While there are some conceptual differences of influential parameters, both methods seek to treat erosion from overland flow exponentially (recall runoff is primarily generated from overland flow). The physics based exponential multiplier was near 1.5 for each of the basins allowing the routine to capture some of the upper end events generated at high flows. These events were routinely underestimated with the MUSLE. Neither routine performed well at replicating upper end events generated by flow and precipitation values near the median of their respective datasets.

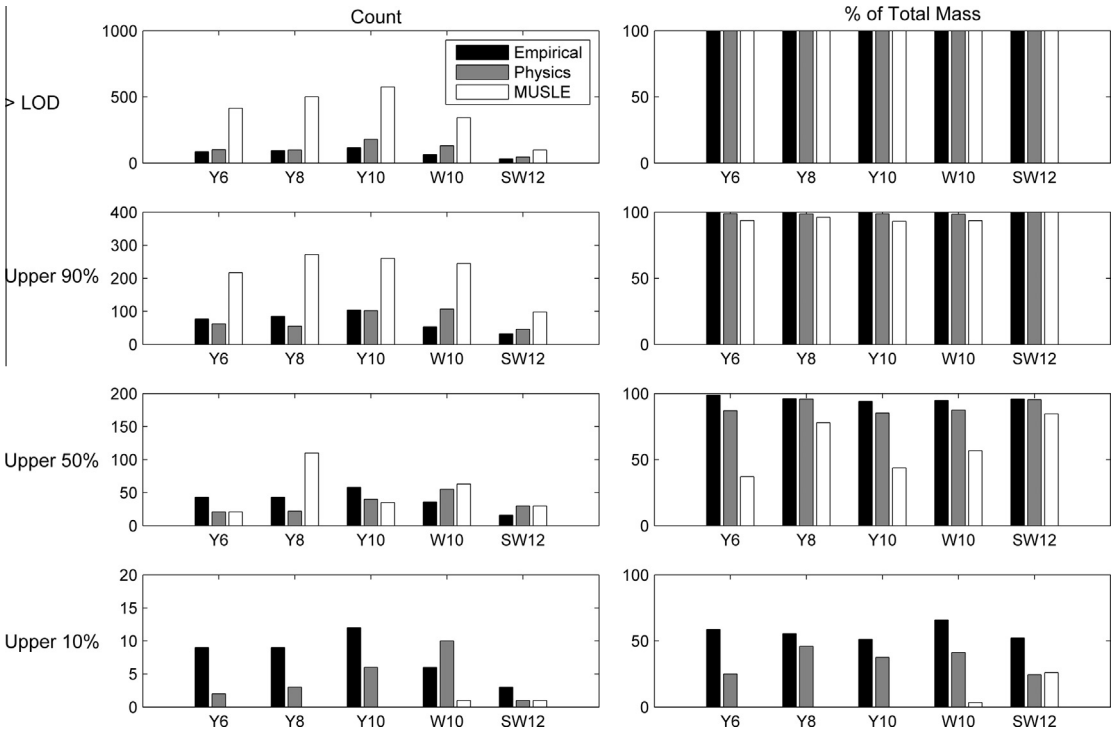

Fig. 8. Erosion days count and percent of total mass at thresholds defined by empirical record (data shown are for validation period).

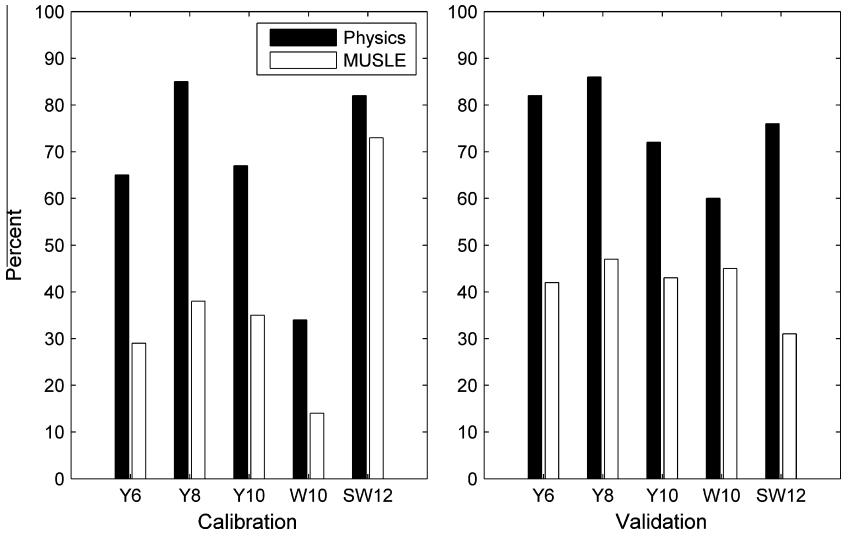

Fig. 9. Percent of total mass captured on days the empirical record indicated erosion.

Both erosion techniques performed similarly in distributing soil losses across seasons holding the same biases as the flow model (underestimation of spring erosion and overestimation of winter erosion). However, examination of model output on individual days when the empirical record indicated erosion showed large discrepancies. Fig. 9 shows the percentage of total mass captured in simulated records on days the empirical record indicated erosion. On average, 40% of the mass estimated with the MUSLE occurred on erosion days compared with 70% through the physics based routine. In other words, over half of the soil loss estimated through the MUSLE occurred on days when the empirical record suggests there was no erosion.

Although long term sums varied little between models, the large differences in erosion event counts and distribution of erosion magnitudes suggests model choice is dependent upon the problem at hand. Model runs indicate the physics based routines are better equipped to apportion mass correctly with respect to upper end events and predict days when erosion would occur. This suggests physics based routines are the best option when event analysis is required. If long term soil loss estimates are needed without specific information on the timing, empirical and physics based models perform similarly.

6. Summary and conclusions

The multidecadal erosion record available at the Riesel watersheds provides the opportunity to examine long-term erosion processes outside of the standard plot setting. The long-term empirical

record (12–51 years) indicates the upper 10% of erosion events comprise roughly half of the long-term soil loss sum. From a return frequency perspective, storms delivering the upper half of the sediment record occurred on average 4–5 times per decade. This relationship was consistent between row crop, native prairie, and hay production unit source watersheds.

Linear regression analysis (single and multiple) indicate daily flow, daily precipitation, and maximum 1 h precipitation are only able to explain about one quarter of the variance in the erosion record. Flow and precipitation values resulting in upper end erosion events ranged from near median values to the upper end of their respective records. Normalizing erosion values by flow, a pattern emerges indicating upper end erosion events are characterized by high erosion indices. Erosion indices were highest during the spring months and during warm season annuals cultivation.

Little difference existed between long-term soil loss estimates using the MUSLE and physics based results. Both routines underestimated long-term soil losses at the row crop basins and were accurate at the hay and prairie watersheds. These results imply either model may be used with similar outcomes if the desired result is an estimate of total long-term erosion at unit-source spatial scales. The study also indicates greater amounts of error will be present in the more highly managed agricultural basins compared to prairie or hay producing areas. Large differences were apparent in the count and distribution of erosion magnitudes between models with the physics based routines performing better.

Acknowledgement

The authors would like to thank agricultural engineer Daren Harmel with the USDA-ARS for help with the data.

References

Aksoy, H., Kavvas, M.L., 2005. A review of hillslope and watershed scale erosion and sediment transport models. Catena 64, 247–271.

Allen, P.B., Welch, N.H., Rhoades, E.D., Edens, C.D., Miller, G.E., 1976. The Modified Chickasha Sediment Sampler. US Department of Agriculture ARS-S-107: pp. 1–17.

Allen, P.M., Harmel, R.D., Arnold, J., Plant, B., Yelderman, J., King, K., 2005. Field data and flow system response in clay (vertisol) shale terrain, north central Texas, USA. Hydrol. Process. 19, 2719–2736. http://dx.doi.org/10.1002/hyp.5782.

Allen, P.M., Harmel, R.D., Dunbar, J.A., Arnold, J.G., 2011. Upland contribution of sediment and runoff during extreme drought: a study of the 1947–1956 drought in the Blackland Praire, Texas. J. Hydrol. 407, 1–11.

Arnold, J.G., Potter, K.N., King, K.W., Allen, P.M., 2005. Estimation of soil cracking and the effect on surface runoff in a Texas Blackland Praire Watershed. Hydrol. Process. 19, 589–603.

Arnold, J.G., Moriasi, D.N., Gassman, P.W., Abbaspour, K.C., White, M.J., Srinivasan, R., Santhi, C., Harmel, R.D., van Griensven, A., van Liew, M.W., Jha, M.K., 2012. SWAT: model use, calibration, and validation. Am. Soc. Agr. Biol. Eng. 55 (4), 1491–1508.

Asquith, W., Slade, R., 1995. Documented and Potential Extreme Peak Discharges and Relation between Potential Extreme Peak Discharges and Probable Maximum Flood Peak Discharges in Texas. USGS Water Resources Investigations Report 95-4249. <http://pubs.usgs.gov/wri/1995/4249/report.pdf>.

Bhuyan, S.J., Kalita, P.K., Janssen, K.A., Barnes, P.L., 2002. Soil loss predictions with three erosion simulation models. Environ. Model. Software 17, 137–146.

Boardman, J., 2006. Soil erosion science: reflections on the limitations of current approaches. Catena 68, 73–86. http://dx.doi.org/10.1016/j.catena.2006.03.007.

Brandt, C.J., 1990. Simulation of the size distribution and erosivity of raindrops and throughfall drops. Earth Surf. Proc. Land. 15 (8), 687–698.

Edwards, W.M., Owens, L.B., 1991. Large storm effects on total soil erosion. J. Soil Water Conserv. 46 (1), 75–78.

Engel, B., Storm, D., White, M., Arnold, J., Arabi, M., 2007. A hydrologic/water quality model application protocol. J. Am. Water Resour. Ass. 43 (5), 1223–1236.

Evans, R., 1995. Some methods of directly assessing water erosion of cultivated land – a comparison of measurements made on plots and in fields. Prog. Phys. Geogr. 19 (1), 115–129.

Gonzalez-Hidalgo, J.C., de Luis, M., Batalla, R.J., 2009. Effects of the largest daily events on total soil erosion by rainwater. An analysis of the USLE database. Earth Surf. Proc. Land. 34, 2070–2077.

Harmel, R.D., King, K.W., Richardson, C.W., Williams, J.R., 2003. Long-term precipitation analyses for the central Texas Blackland Prarie. Trans. Am. Soc. Agr. Eng. 46 (5), 1381–1388.

Harmel, R.D., Richardson, C.W., King, K.W., Allen, P.M., 2006. Runoff and soil loss relationships for the Texas Blackland Prairies ecoregion. J. Hydrol. 331, 471–483.

Harmel, R.D., Bonta, J.V., Richardson, C.W., 2007. The original USDA-ARS experimental watersheds in Texas and Ohio: contributions from the past and visions for the future. Trans. Am. Soc. Agr. Biol. Eng. 50 (5), 1669–1675.

Harmel, R.D., Smith, D.R., King, K.W., Slade, R.M., 2009. Estimating storm discharge and water quality data uncertainty: a software tool for monitoring and modeling applications. Environ. Model. Software 24 (7), 832–842.

Jeong, J., Kannan, N., Arnold, J., Glick, R., Gosselink, L., Srinivasan, R., 2010. Development and integration of sub-hourly rainfall-runoff modeling capability within a watershed model. Water Resour. Manage 24, 4505–4527. http://dx.doi.org/10.1007/s11269-010-9670-4.

Jeong, J., Kannan, N., Arnold, J.G., Glick, R., Gosselink, L., Srinivasan, R., Harmel, R.D., 2011. Development of sub-daily erosion and sediment transport algorithms for SWAT. Trans. Agr. Biol. Eng. 54 (5), 1685–1691.

Kohler, M.A., Linsley, R.K., 1951. Predicting the Runoff from Storm Rainfall. Weather Bureau, US Department of Commerce, Research Paper, No. 34, Washington DC: pp. 1–9.

Lane, L.J., Kidwell, M.R., 2003. Hydrology and Soil Erosion. USDA Forest Service Proceeding RMRS-P-30. pp. 92–100.

Merritt, W.S., Letcher, R.A., Jakeman, A.J., 2003. A review of erosion and sediment transport models. Environ. Model. Software 18, 761–799.

Morgan, R.P.C., Quinton, J.N., Smith, R.E., Govers, G., Poesen, J.A., Auerswald, K., Chisci, G., Torri, D., Styczen, M.E., 1998. The European soil erosion model (EUROSEM): a process-based approach for predicting sediment transport from fields and small catchments. Earth Surf. Proc. Land. 23, 527–544.

Moriasi, D.N., Arnold, J.G., van Liew, M.W., Binger, R.L., Harmel, R.D., Veith, T., 2007. Model evaluation guidelines for systematic quantification of accuracy in watershed simulations. Trans. Am. Soc. Agr. Biol. Eng. 50 (3), 885–900.

Nearing, M.A., 1998. Why soil erosion models over-predict small soil losses and under-predict large soil losses. Catena 32, 15–22.

Nearing, M.A., 2000. Evaluating soil erosion models using measured plot data: accounting for variability in the data. Earth Surf. Proc. Land. 25, 1035–1043.

Nearing, M.A., 2013. Soil erosion and conservation. In: Wainwright, J., Mulligan, M. (Eds.), Environmental Modelling: Finding Simplicity in Complexity 2nd Edition. pp. 365–378.

Nearing, M.A., Foster, G.R., Lane, L.J., Finkner, S.C., 1989. A process-based soil erosion model for USDA-water erosion prediction project technology. Trans. Am. Soc. Agr. Eng. 32 (5), 1587–1593.

Nearing, M.A., Nichols, M.N., Stone, J.J., Renard, K.G., Simanton, J.R., 2007. Sediment yields from unit-source semiarid watersheds at Walnut Gulch. Water Resour. Res. 43, W06426. http://dx.doi.org/10.1029/2006WR005692.

Neitsch, S.L., Arnold, J.G., Kiniry, J.R., Williams, J.R., 2011. Soil and Water Assessment Tool, User Manual, Version 2009. Temple, Tx: Grassland, Soil and Water Research Laboratory.

Renard, K.G., Foster, G.R., Weesies, G.A., et al., 1997. Predicting Soil Erosion by Water – A Guide to Conservation Planning with the Revised Universal Soil Loss Equation (RUSLE), Agricultural Handbook No. 703, US Government Printing Office, Washington DC.

Risse, L.M., Nearing, M.A., Nicks, A.D., Laflen, J.M., 1993. Assessment of error in the universal soil loss equation. Soil Sci. Soc. Am. J. 57, 825–833.

Ruttimann, M., Schaub, D., Prasuhn, V., Reugg, W., 1995. Measurement of runoff and soil erosion on regularly cultivated fields in Switzerland – some critical considerations. Catena 25, 127–139.

Shih, H., Yang, C.T., 2009. Estimating overland flow erosion capacity using unit stream power. Int. J. Sedim. Res. 24, 46–62.

Smith, R.E., 1981. A kinematic model for surface mine sediment yield. Trans. Am. Soc. Agr. Biol. Eng. 24 (6), 1508–1514.

Tiwari, A.K., Risse, L.M., Nearing, M.A., 2000. Evaluation of WEPP and its comparison with USLE and RUSLE. Trans. Am. Soc. Agr. Biol. Eng. 43 (5), 1129–1135.

Wang, X., Harmel, R.D., Williams, J.R., Harman, W.L., 2006. Evaluation of EPIC for assessing crop yield, runoff, sediment and nutrient losses from watersheds with poultry litter fertilization. Trans. Am. Soc. Agr. Biol. Eng. 49 (1), 47–59.

Wendt, R.C., Alberts, E.E., Hjelmfelt, A.T., 1986. Variability of runoff and soil loss from fallow experimental plots. Soil Sci. Soc. Am. J. 50, 730–736.

White, S., 2005. Sediment yield prediction and modeling. Hydrol. Process. 19, 3053–3057.

Williams, J.R., 1975. Sediment routing for agricultural watersheds. Water Resour. Bull. 11 (5), 965–974.

Williams, J.R., Arnold, J.G., Kiniry, J.R., Gassman, P.W., Green, C.H., 2008. History of model development at Temple, Texas. Hydrol. Sci. 53 (5), 948–960.

Wischmeier, W.H., Smith, D.D., 1978. Predicting Rainfall Erosion Losses – A Guide to Conservation Planning, Agricultural Handbook No. 537, US Government Printing Office, Washington DC.